CHEMISTRY
A EUROPEAN JOURNAL

REVIEWS

Natural Products

*O. Chantarasriwong, A. Batova, W. Chavasiri, E. A. Theodorakis** ..... 9944 – 9962

Chemistry and Biology of the Caged *Garcinia* Xanthones

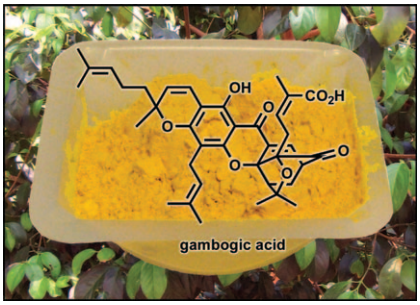

Golden discovery: Gamboge, the golden resin of various *Garcinia* trees, has a spectacular history in traditional Asian medicine. Chemical analysis of gamboge led to the identification of a new family of bioactive metabolites collectively referred to as caged *Garcinia* xanthones. Represented by gambogic acid (see figure), this family is highlighted by a privileged chemical scaffold that holds remarkable potential in chemistry, biology, and medicine.

COMMUNICATIONS

Metal-Mediated Synthesis

R. Campbell, P. García-Álvarez, A. R. Kennedy, R. E. Mulvey** ..... 9964 – 9968

Synergic Transformation of an Ethylenediamine to a Lithium 1,3-Diaza-2-zincacyclopentene via an Alkyllithium/Bis(alkyl)zinc Mixture

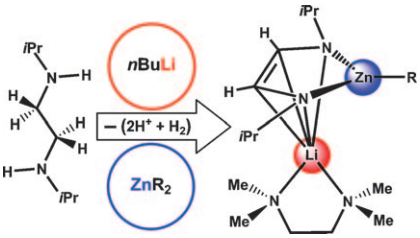

Deadly duo: Four bonds in total, two N–H and two C–H bonds, have been cleaved from a neutral secondary diamine through the cooperative effects of a lithium alkyl–zinc bisalkyl coalition aided by *N*,*N*,*N*′,*N*′-tetramethylethylenediamine (TMEDA) to generate a dianionic diazaethene (see scheme).

Asymmetric Catalysis

*K. Zheng, Y. Yang, J. Zhao, C. Yin, L. Lin, X. Liu, X. Feng** ... 9969 – 9972

The Magnesium(II)-Catalyzed Asymmetric Ketone–Ene Reaction under Solvent-Free Conditions: Stereocontrolled Access to Enantioenriched Trifluoromethyl-Substituted Compounds

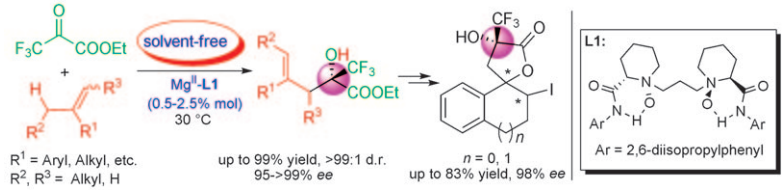

Salt of the (alkaline) earth: A highly efficient asymmetric ketone–ene reaction of trifluoropyruvate catalyzed by a chiral $Mg(OTf)_2$–*N*,*N*′-dioxide complex is described (see scheme). The catalyst system exhibits a broad substrate scope and the trifluoromethylated α-hydroxy esters were obtained under solvent-free conditions. The C=C bond of the products offers a handle for further transformations and trifluoromethyl-substituted spirocyclic compounds were synthesized in excellent *ee* and high yield.

Oxidation

P. Cordier, C. Aubert, M. Malacria, V. Gandon,* E. Lacôte** .... 9973 – 9976

Oxidation of α-Alkoxy Allenes into α′-Alkoxy Enones

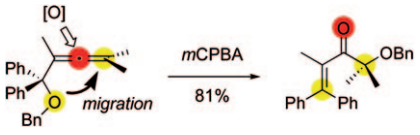

Rearrangement enablers: α-Alkoxy allenes undergo regioselective oxidative migration to give α′-alkoxy enones in good to excellent yields (see scheme; Bn = benzyl, *m*CPBA = *m*-chloroperbenzoic acid). The influence of substituents on the allene, at C1, and at the oxygen atom has been examined. In addition, an oxidative cascade delivers α′-alkoxy oxiranyl ketones through diepoxidation.

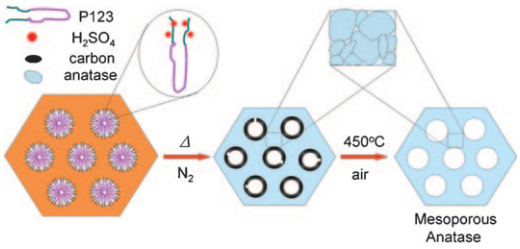

Mesoporous Materials

*R. Y. Zhang, B. Tu, D. Y. Zhao** ..... 9977 – 9981

Synthesis of Highly Stable and Crystalline Mesoporous Anatase by Using a Simple Surfactant Sulfuric Acid Carbonization Method

Highly stable and crystalline mesoporous TiO_2 materials have been successfully synthesized by a simple surfactant sulfuric acid carbonization method by using Pluronic triblock copolymers as a template (see figure). The surfactant template is first carbonized by H_2SO_4 to obtain rigid carbon on the surface of mesochannels that can then support the mesostructure during crystallization at high temperatures.

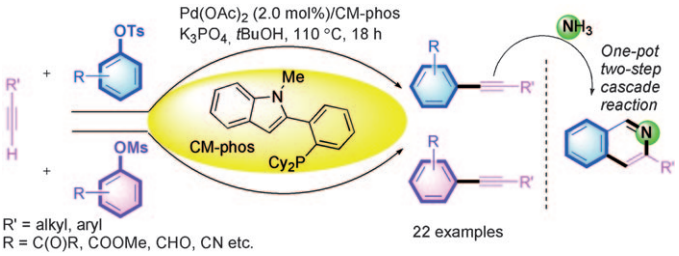

Cross-Coupling

*P. Y. Choy, W. K. Chow, C. M. So, C. P. Lau, F. Y. Kwong** .... 9982 – 9985

Palladium-Catalyzed Sonogashira Coupling of Aryl Mesylates and Tosylates

Up to speed: The first general and mild protocol for the Sonogashira coupling of aryl mesylates is presented (see scheme). The coupling intermediate also provides facile access to 2-substituted isoquinolines.

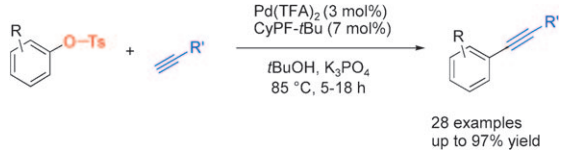

Cross-Coupling

O. R'kyek, N. Halland, A. Lindenschmidt, J. Alonso, P. Lindemann, M. Urmann, M. Nazaré** ..... 9986 – 9989

A General Palladium-Catalyzed Sonogashira Coupling of Aryl and Heteroaryl Tosylates

Coupled up: A new general palladium-catalyzed procedure for the cross-coupling of aryl and heteroaryl tosylates is described. This highly versatile and efficient process can be used for the synthesis of a wide variety of functionalized alkynes (see scheme).

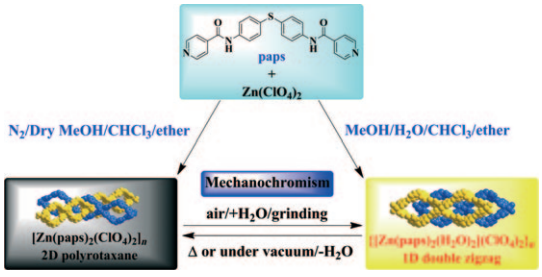

Coordination Frameworks

B.-C. Tzeng, T.-Y. Chang, H.-S. Sheu* ..... 9990 – 9993

Reversible Phase Transformation and Luminescent Mechanochromism of Zn^{II}-Based Coordination Frameworks Containing a Dipyridylamide Ligand

It's all in the grinding: A 1D double-zigzag framework, $\{[Zn(paps)_2(H_2O)_2](ClO_4)_2\}_n$, was synthesized by the reaction of $Zn(ClO_4)_2$ with paps (see structure in scheme) in a layer method. A similar reaction, but in which dry solvents were used instead, led to the formation of a 2D polyrotaxane framework, $[Zn(paps)_2(ClO_4)_2]_n$. Both structures can be interconverted by heating and grinding in the presence of moisture and a remarkable luminescent mechanochromism in the transformation process is also observed by monitoring their luminescence images.

Magnetic Properties

B. Zhang, D. Zhu,* Y. Zhang* ..... 9994 – 9997

Crystal-to-Crystal Transformation from a Mononuclear Compound in a Hydrogen-Bonded Three-Dimensional Framework to a Layered Coordination Polymer

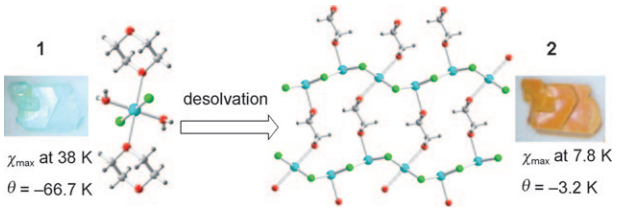

Out of the blue: Blue crystals composed of a mononuclear compound in a hydrogen-bonded three-dimensional framework (**1**) can be transformed into brown crystals composed of a layered coordination polymer (**2**) by desolvation (see figure). These crystal-to-crystal transformations result in changes in the dimensionality, color, and physical properties.

FULL PAPERS

Coordination Chemistry

*J. R. Neilson, J. A. Kurzman, R. Seshadri, D. E. Morse** 9998 – 10006

Cobalt Coordination and Clustering in α-Co(OH)$_2$ Revealed by Synchrotron X-ray Total Scattering

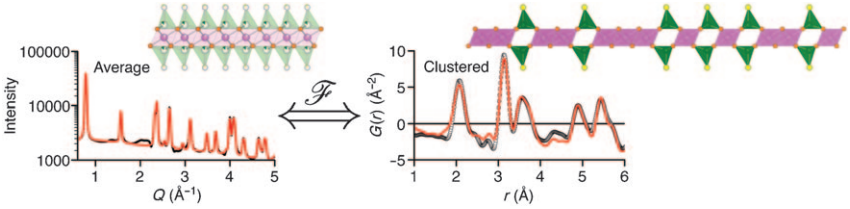

Local structure—cobalt clustering: The structures of layered hydroxides are not well described by traditional crystallography. Total scattering of a particular subset of these materials reveals that different cobalt coordination polyhedra cluster within each layer (see graphic) on short length scales, offering new insights into approaches for understanding the properties of layered materials.

Nanocatalysts

D. Wang, A. Villa, P. Spontoni, D. S. Su,* L. Prati* ..... 10007 – 10013

In Situ Formation of Au–Pd Bimetallic Active Sites Promoting the Physically Mixed Monometallic Catalysts in the Liquid-Phase Oxidation of Alcohols

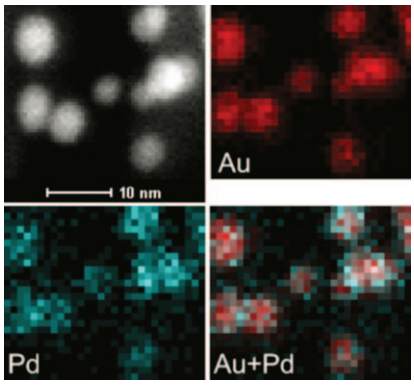

Active alloys: Starting from a physical mixture of Au/AC and Pd/AC catalysts (AC = activated carbon), an Au–Pd alloy can be formed during the liquid-phase oxidation of alcohols by reprecipitation of Pd onto Au nanoparticles (see images). The alloy formation greatly enhances the catalyst activity.

Polyoxometalates

*I. Kaminker, H. Goldberg, R. Neumann, D. Goldfarb** ..... 10014 – 10020

High-Field Pulsed EPR Spectroscopy for the Speciation of the Reduced [PV$_2$Mo$_{10}$O$_{40}$]$^{6-}$ Polyoxometalate Catalyst Used in Electron-Transfer Oxidations

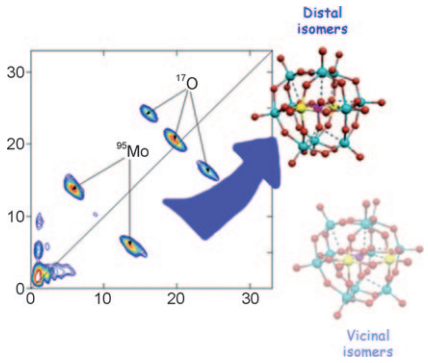

A band apart: A W-band EPR study of [PV^{IV}V^{V}Mo$_{10}$O$_{40}$]$^{6-}$ was carried out. Two species related to [PV^{IV}V^{V}Mo$_{10}$O$_{40}$]$^{6-}$ were identified. One is vanadyl (VO^{2+})-like and is represented as an ion pair, [PV^{V}Mo$_{10}$O$_{39}$]$^{8-}$[V^{IV}O]$^{2+}$; the other originates from reduction of distal H$_5$PV$_2$Mo$_{10}$O$_{40}$ isomers to yield an intact cluster, [PV^{IV}V^{V}Mo$_{10}$O$_{40}$]$^{6-}$ (see graphic).

CONTENTS

Eight is better than one: Photophysical characterisation of a series of novel phthalocyanine–perylene "octad" molecules shows rapid energy transfer, rather than the anticipated charge separation process, upon photoexitation (see figure).

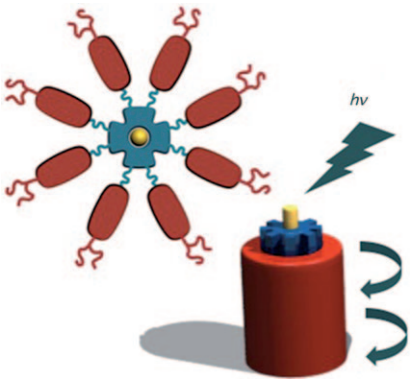

Delocalised States

S. Albert-Seifried, C. E. Finlayson, F. Laquai, R. H. Friend, T. M. Swager, P. H. J. Kouwer,* M. Juríček, H. J. Kitto, S. Valster, R. J. M. Nolte, A. E. Rowan* ..... 10021 – 10029

Multichromophoric Phthalocyanine–(Perylenediimide)$_8$ Molecules: A Photophysical Study

Caught in a trap! The two L-isomers of 3-fluoroaspartate were synthesized and used to probe pyruvoyl-dependent aspartate decarboxylase enzymes. Our results show that these molecules maintain their unique conformations (as determined by the presence of fluorine) even in the active site of these enzymes, leading to differentiated reactivity and binding profiles and, in one case, a stable enzyme/product complex (see figure).

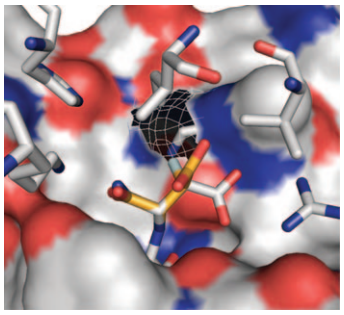

Fluorinated Inhibitors

*J. de Villiers, L. Koekemoer, E. Strauss** ..... 10030 – 10041

3-Fluoroaspartate and Pyruvoyl-Dependant Aspartate Decarboxylase: Exploiting the Unique Characteristics of Fluorine To Probe Reactivity and Binding

Let there be light: The plasmonic photocatalyst Ag@Ag(Br,I) has been fabricated by the ion-exchange process and light-induced chemical reduction reaction. The photocatalytic properties of the sample were evaluated by photoreducing Cr^{VI} and photooxidizing methylic orange (MO) under visible light (reaction arrows in red and green refer to two separate processes).

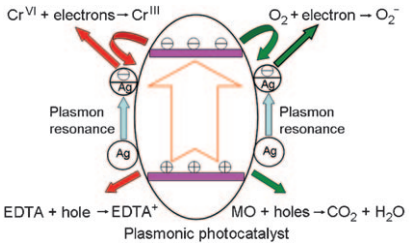

Photocatalysis

P. Wang, B. Huang, Q. Zhang, X. Zhang, X. Qin, Y. Dai, J. Zhan, J. Yu, H. Liu, Z. Lou* .... 10042 – 10047

Highly Efficient Visible Light Plasmonic Photocatalyst Ag@Ag(Br,I)

Taking control: MCM-41 mesoporous materials have been prepared that contain $[Ru(bipy)_3]Cl_2$ (bipy = bipyridine) inside the mesopores and anion binding groups (i.e., imidazolium, urea and thiourea) in the pore outlets. The delivery of these materials in the presence of long-chain carboxylate ions and anionic surfactants has been studied. Molecular dynamic simulations that use force-field methods have been made to theoretically study the capping carboxylate mechanism (see scheme).

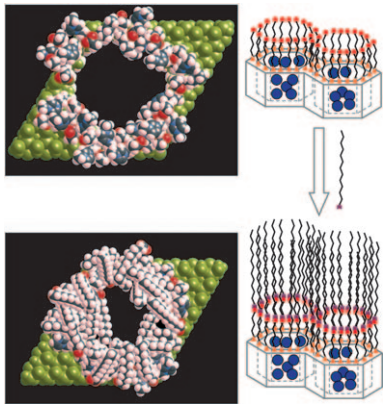

Hybrid Materials

C. Coll, E. Aznar, R. Martínez-Máñez, M. D. Marcos, F. Sancenón,* J. Soto, P. Amorós, J. Cano, E. Ruiz* ..... 10048 – 10061

Fatty Acid Carboxylate- and Anionic Surfactant-Controlled Delivery Systems That Use Mesoporous Silica Supports

Molecular Machines

*E. Busseron, C. Romuald, F. Coutrot** ..... 10062 – 10073

Bistable or Oscillating State Depending on Station and Temperature in Three-Station Glycorotaxane Molecular Machines

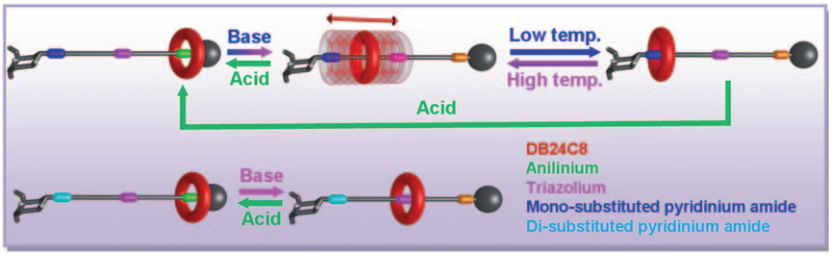

Three molecular stations with different affinity for dibenzo[24]crown-8 (DB24C8) are present in the glycorotaxane molecular machines shown schematically in the picture. At low pH, DB24C8 resides around the best anilinium station, whereas at higher pH, the macrocycle behaves very differently depending on the substitution of the pyridinium amide station and on the temperature (bistable or oscillating state).

Spin Crossover

S. Thies, C. Bornholdt, F. Köhler, F. D. Sönnichsen, C. Näther, F. Tuczek, R. Herges** . . 10074 – 10083

Coordination-Induced Spin Crossover (CISCO) through Axial Bonding of Substituted Pyridines to Nickel–Porphyrins: σ-Donor versus π-Acceptor Effects

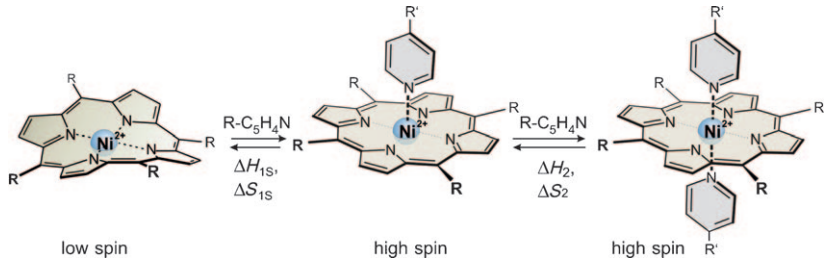

In a spin: Nickel–porphyrin (R = C_6F_5) coordinates two axial pyridine ligands upon changing from the $S=0$ to the $S=1$ state. The association constants of both steps correlate with the pK_a of the pyridines but the binding enthalpies and entropies do not. Back donation from nickel to the electron-deficient pyridines (see picture) leads to an increase in association enthalpy and a shift of IR stretching frequencies in the corresponding pyridines to lower wavenumbers.

Supramolecular Chemistry

*M. R. Molla, A. Das, S. Ghosh** ..... 10084 – 10093

Self-Sorted Assembly in a Mixture of Donor and Acceptor Chromophores

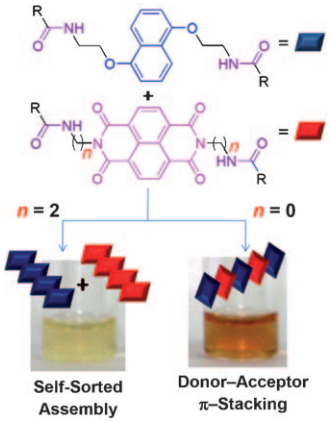

Self-assembly in a true sense: Self-sorted assembly in a mixture of bis-amide-functionalised donor and acceptor chromophores has been achieved due to the synergistic effect of π–π stacking and hydrogen bonding. Remarkable differences in the mode of self-assembly (self-sorting vs. donor–acceptor π stacking, see figure) was noticed, depending on the position of the amide functionalities with respect to the individual chromophores.

CONTENTS

Dual probes for cellular imaging: A novel bimodal medium-sized fluorescence/MRI probe based on a cyclodextrin scaffold has been synthesized and characterized (illustrated schematically here). This new Gd^{III} contrast agent, exhibiting a high relaxivity confined to a small molecular space ($r_1 \approx 150\ s^{-1}\,mM^{-1}$ per molecule of contrast agent), has been successfully used for the imaging of pancreatic islets and stem cells.

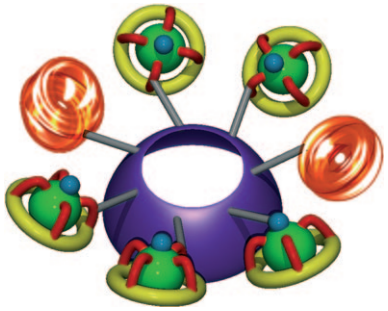

Contrast Agents

Z. Kotková, J. Kotek, D. Jirák, P. Jendelová, V. Herynek, Z. Berková, P. Hermann, I. Lukeš* .... 10094 – 10102

Cyclodextrin-Based Bimodal Fluorescence/MRI Contrast Agents: An Efficient Approach to Cellular Imaging

The Midas touch: Core etching of gold nanoparticles by bovine serum albumin (BSA) results in quantum clusters (QCs), the luminescence of which (see picture) is exploited as a "turn-off" sensor for the detection of Cu^{2+} ions and a "turn-on" sensor for glutathione detection. Metal-enhanced luminescence of the QCs occurs in the presence of silver nanoparticles. The luminescence of Au_{QC}@BSA is used for imaging carcinoma cells by folic acid mediated endocytosis.

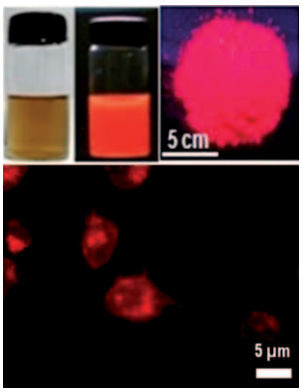

Quantum Clusters

M. A. Habeeb Muhammed, P. K. Verma, S. K. Pal, A. Retnakumari, M. Koyakutty, S. Nair, T. Pradeep ..... 10103 – 10112

Luminescent Quantum Clusters of Gold in Bulk by Albumin-Induced Core Etching of Nanoparticles: Metal Ion Sensing, Metal-Enhanced Luminescence, and Biolabeling

Silver mining: Aniline–sulfoanisidine copolymer nanosorbents demonstrate ultrastrong adsorbability and highly efficient recovery of Ag^I from waste water in the form of separable silver nanocrystals, turning trash into treasure. The maximal Ag^I sorption capacity of 2034 $mg\,g^{-1}$ (18.86 $mmol\,g^{-1}$) is the highest so far, and at $\leq$2 mM Ag^I, the nanosorbent exhibits $\geq$99.98% Ag^I adsorptivity. The picture shows the possible sorption mechanism, as well as XRD and microscopy evidence for the presence of elemental silver in the Ag-loaded nanosorbent.

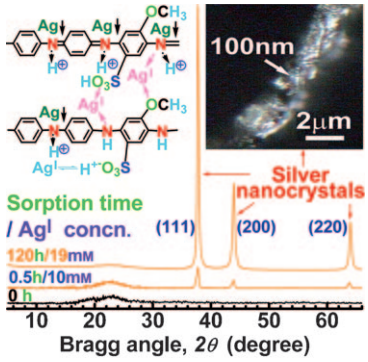

Nanosorbents

X.-G. Li, H. Feng, M.-R. Huang** ..... 10113 – 10123

Redox Sorption and Recovery of Silver Ions as Silver Nanocrystals on Poly(aniline-*co*-5-sulfo-2-anisidine) Nanosorbents

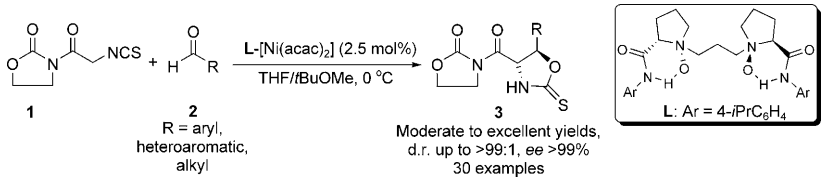

A nickel for your thoughts: A chiral *N*,*N*′-dioxide–nickel(II) complex has been applied in the asymmetric direct aldol reaction of α-isothiocyanato imide with aldehydes. A series of aromatic, α,β-unsaturated, heteroaromatic, and aliphatic aldehydes were converted into the desired β-hydroxy-α-amino acid derivatives under mild conditions (see scheme). A possible transition state has been proposed.

Asymmetric Synthesis

*X. Chen, Y. Zhu, Z. Qiao, M. Xie, L. Lin, X. Liu, X. Feng** 10124 – 10129

Efficient Synthesis of β-Hydroxy-α-Amino Acid Derivatives via Direct Catalytic Asymmetric Aldol Reaction of α-Isothiocyanato Imide with Aldehydes

Asymmetric Catalysis

*Z. Wang, D. Chen, Z. Yang, S. Bai, X. Liu, L. Lin, X. Feng** 10130 – 10136

Highly Enantioselective Synthesis of α-Stereogenic Esters through Catalytic Asymmetric Michael Addition of 4-Oxo-4-arylbutenoates

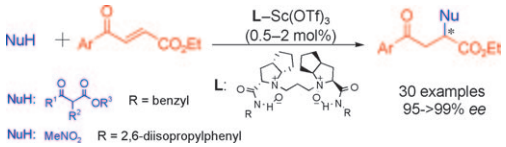

Add it up: Highly enantioselective Michael addition of 1,3-dicarbonyl compounds and nitromethane to 4-oxo-4-arylbutenoates catalyzed by *N,N′*-dioxide–$Sc(OTf)_3$ complexes have been developed (see scheme). Various α-stereogenic esters were obtained regioselectively with excellent yields and enantioselectivities under mild conditions.

Homogeneous Catalysis

*C. Mukherjee, A. Stammler, H. Bögge, T. Glaser** ..... 10137 – 10149

Do Trinuclear Triplesalen Complexes Exhibit Cooperative Effects? Synthesis, Characterization, and Enantioselective Catalytic Sulfoxidation by Chiral Trinuclear Fe^{III} Triplesalen Complexes

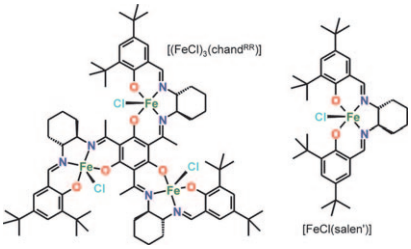

Complex chemistry: The reaction of the trinuclear chiral triplesalen complex $[(FeCl)_3(chand^{RR})]$ in the enantioselective catalytic sulfoxidation of prochiral sulfides has altered cooperative effects through the central phloroglucinol backbone relative to the mononuclear analogue [FeCl(salen′)].

Total Synthesis

Y. Hayashi, H. Yamaguchi, M. Toyoshima, K. Okado, T. Toyo, M. Shoji* ..... 10150 – 10159

Formal Total Synthesis of Fostriecin by 1,4-Asymmetric Induction with an Alkyne–Cobalt Complex

CoCo catalysis: Four stereogenic centers and a conformationally labile *cis-cis-trans*-triene moiety were constructed in a formal total synthesis of fostriecin. The synthesis incorporates the first successful example of the use of an alkyne–cobalt complex in 1,4-asymmetric induction.

Bonding Analysis

*S. Klein, R. Tonner, G. Frenking** ..... 10160 – 10170

Carbodicarbenes and Related Divalent Carbon(0) Compounds

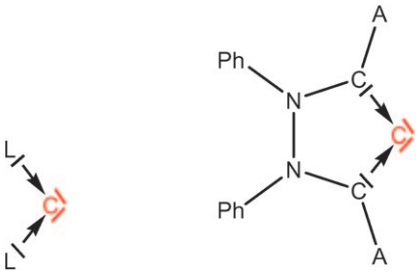

Carbene or carbone? Quantum-chemical studies on dicoordinated carbon compounds with various mono- and bidentate ligands (see picture) show that there is a gliding scale between the bonding situation of carbenes R–C–R, in which the carbon atom has one electron pair, and carbones L→C←L, in which the carbon atom has two electron pairs. Divalent carbon(0) compounds (carbones) CL_2 are π donors, whereas divalent carbon(II) compounds (carbenes) CR_2 are π acceptors.

Radical Reactions

*M. Lüthy, K. Schenk, P. Renaud** ..... 10171 – 10177

Synthesis of Unusual Oxime Ethers by Reaction of Tetranitromethane with *B*-Alkylcatecholboranes

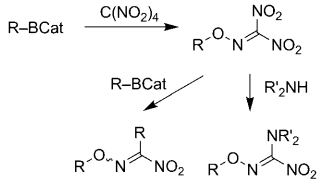

Radical addition: *B*-Alkylcatecholboranes were found to react spontaneously, through a radical pathway, with tetranitromethane to afford dinitrooxime ethers. Further substitution of one of the nitro groups in the oxime ethers by alkyl radicals and nucleophiles is also reported (see scheme).

CONTENTS

Frozen magnetisation: The relaxation time of Fe_4 single-molecule magnets increases upon going from the solid state to a frozen solution. The effective energy barrier for relaxation of the magnetisation and the magnetic anisotropy are unchanged, but the Arrhenius prefactor is strongly enhanced.

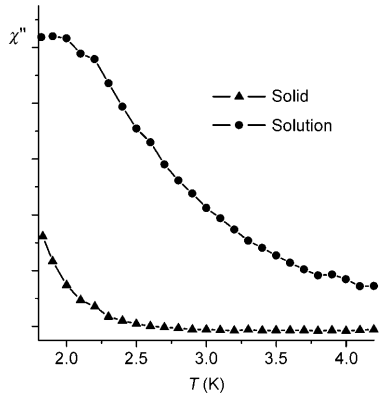

Magnetic Properties

C. Schlegel, E. Burzurí, F. Luis, F. Moro, M. Manoli, E. K. Brechin, M. Murrie, J. van Slageren ..... 10178 – 10185

Magnetic Properties of Two New Fe_4 Single-Molecule Magnets in the Solid State and in Frozen Solution

Enhancement through confinement: A nano-enzyme reactor has been constructed that can monitor the product from an enzymatic reaction in situ (see scheme; Glu = glucose, GOD = glucose oxidase, PAA = porous anodic alumina). The activity and stability of the enzyme confined in the nanochannel space are enhanced. In addition, the enzymatic reaction changes from a process controlled by mass transport at low flux to a process controlled by enzymatic reaction kinetics at high flux (e.g., $>50\ \mu L\,min^{-1}$).

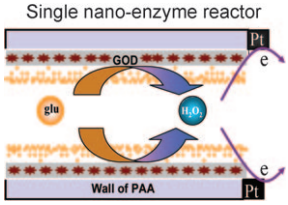

Nanobioreactors

S.-J. Li, C. Wang, Z.-Q. Wu, J.-J. Xu, X.-H. Xia, H.-Y. Chen* .. 10186 – 10194

Real-Time Monitoring of Mass-Transport-Related Enzymatic Reaction Kinetics in a Nanochannel-Array Reactor

Solvent-dependent catalysis: A new diphenylphosphane, based on the β-cyclodextrin (CD) skeleton, exhibits dual solubility and a solvent-dependent conformation change in which the self-inclusion of a phenyl group of the phosphane moiety into the CD cavity, observed in water, disappears in organic solvents (see scheme). Hydrogenation or hydroformylation reactions were performed in both water and organic solvents.

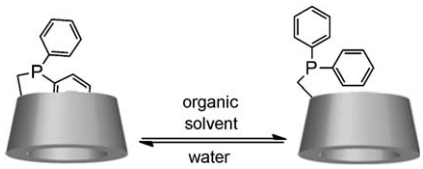

Host–Guest Catalysis

C. Machut-Binkowski, F.-X. Legrand, N. Azaroual, S. Tilloy, E. Monflier* ..... 10195 – 10201

New Phosphane Based on a β-Cyclodextrin, Exhibiting a Solvent-Tunable Conformation, and its Catalytic Properties

Turning the knob: 2,6-Bis(1,2,3-triazol-4-yl)pyridine (see figure) ligands with substitution patterns ranging from strongly electron-donating to strongly electron-accepting groups, readily prepared by means of Cu-catalyzed 1,3-dipolar cycloaddition ("click" reaction), were investigated with regard to their complexation behavior, and the properties of the resulting transition-metal complexes were compared.

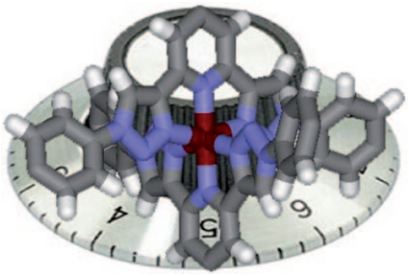

Click Chemistry

M. Ostermeier, M.-A. Berlin, R. M. Meudtner, S. Demeshko, F. Meyer, C. Limberg, S. Hecht* ..... 10202 – 10213

Complexes of Click-Derived Bistriazolylpyridines: Remarkable Electronic Influence of Remote Substituents on Thermodynamic Stability as well as Electronic and Magnetic Properties

Alkaloids

A. Lesarri, E. J. Cocinero, L. Evangelisti, R. D. Suenram, W. Caminati, J.-U. Grabow* ..... 10214 – 10219

The Conformational Landscape of Nicotinoids: Solving the Conformational Disparity of Anabasine

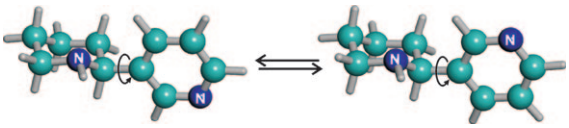

Nicotinoid stereochemistry: The two most stable conformations of free anabasine (eq-eq-*syn*, left, and eq-eq-*anti*, right; eq = equatorial) have been characterized in a jet expansion by using rotational spectroscopy.

Nanowires

G. Wang, Y. Deng,* L. Guo** ..... 10220 – 10225

Single-Crystalline ZnO Nanowire Bundles: Synthesis, Mechanism and Their Application in Dielectric Composites

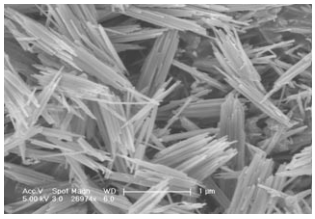

A facile synthesis route has been designed for selective syntheses of uniform single-crystalline ZnO nanowire bundles (see figure). The ZnO bundles/poly(vinylidene fluoride) composites have significantly higher dielectric constants than those of bulk ZnO/poly(vinylidene fluoride) with a quite low percolation threshold.

Self-Assembly

E. Besson, A. Mehdi, A. Van der Lee, H. Chollet, C. Reyé, R. Guilard, R. J. P. Corriu* ..... 10226 – 10233

Selective Lanthanides Sequestration Based on a Self-Assembled Organosilica

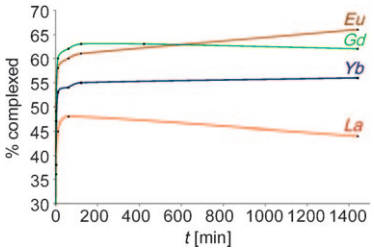

A bis-zwitterionic lamellar material containing ammonium carboxylate groups was tested for cation-exchange properties. It was found to be selective towards lanthanides; cation uptake was dependent on the nature of the $LnCl_3$ salt (Ln = La, Eu, Tb, Er and Yb; see figure).

Nanotechnology

*Q. Zhang, W. Li, L.-P. Wen, J. Chen, Y. Xia** ..... 10234 – 10239

Facile Synthesis of Ag Nanocubes of 30 to 70 nm in Edge Length with CF_3COOAg as a Precursor

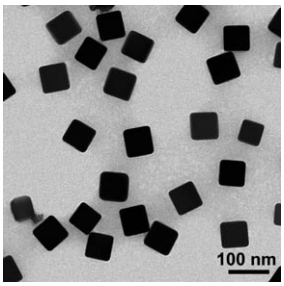

New protocol: We describe a new protocol to synthesize Ag nanocubes of 30 to 70 nm in edge length (see figure) with the use of CF_3COOAg as a precursor to elemental silver. By adding a trace amount of NaSH and HCl to the polyol synthesis, Ag nanocubes were obtained with good quality, high reproducibility, and on a scale of up to 0.19 g per batch for the 70 nm Ag nanocubes.

Radical Reactions

*K. D. Collins, J. M. Oliveira, G. Guazzelli, B. Sautier, S. D. Grazia, H. Matsubara, M. Helliwell, D. J. Procter** ..... 10240 – 10249

Selective Reductions of Cyclic 1,3-Diesters by Using SmI_2 and H_2O

Under water control: The activation of SmI_2 with H_2O allows the carbonyl groups of cyclic 1,3-diesters to be reduced with high chemoselectivity. The radicals formed in the reduction have been exploited in diastereoselective intramolecular additions to alkenes.

CONTENTS

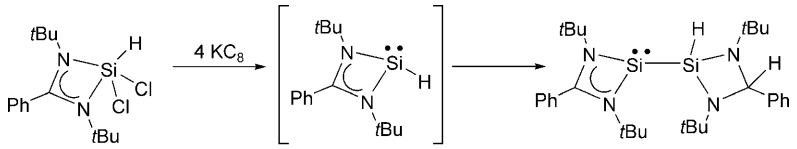

Silylsilylenes on rare form: Monomeric silylsilylene **2** was synthesized by treating **1** with potassium graphite. The reaction proceeds through an intermediate silicon(II) hydride that undergoes a hydrosilylation with the amidinate of another silicon(II) hydride to form **2** (see scheme). The existence of the silicon(II) hydride was shown by the treatment of [{PhC(N*t*Bu)$_2$}SiCl] with [K{HB(*i*Bu)$_3$}]. The structure of **2** has been determined by X-ray crystallography and DFT calculations.

Hydrosilylation

*S.-H. Zhang, H.-X. Yeong, H.-W. Xi, K. H. Lim, C.-W. So** .... 10250 – 10254

Hydrosilylation of a Silicon(II) Hydride: Synthesis and Characterization of a Remarkable Silylsilylene

* Author to whom correspondence should be addressed

Supporting information on the WWW (see article for access details).

VIP Full Papers labeled with this symbol have been judged by two referees as being "very important papers".

A video clip is available as Supporting Information on the WWW (see article for access details).

SERVICE

Spotlights 9938 **Author Index** 10256 **Keyword Index** 10257 **Preview** 10259

CORRIGENDUM

*S. Vargas, A. Suárez, E. Álvarez, A. Pizzano** 9856–9859

Highly Enantioselective Hydrogenation of Enol Ester Phosphonates: A Versatile Procedure for the Preparation of Chiral β-Hydroxyphosphonates

Chem. Eur. J., **2008**, *14*

DOI: 10.1002/chem.200801588

In their Communication, the authors have found errors in Tables 1 and 2. The enantioselectivity of product **2a** (Table 1, entry 4) was 99% *ee* and not 59% *ee*. The reaction time for the reactions in Table 2, entries 4–8 was 72 h. The authors sincereley apologize for these errors and any inconvenience they may have caused.